ELSEVIER Nuclear Instruments and Methods in Physics Research A 418 (1998) 22–31

NUCLEAR INSTRUMENTS & METHODS IN PHYSICS RESEARCH Section A

Status of the OPAL microvertex detector and new radiation monitoring and beam dump system

Sijbrand de Jong*

Indiana University, Physics Department, Swain Hall West 117, Bloomington, IN 47405, USA

Representing the OPAL microvertex group

Abstract

The status of the OPAL Phase III microvertex detector is discussed briefly. This is followed by a more detailed description of the OPAL microvertex detector radiation monitoring and beam dump system. This system measures AC currents induced by radiation on each passing of the beams in silicon diodes mounted close to the microvertex detector front-end electronics. Examples are shown for incidents leading to a beam dump trigger. The integrated radiation dose is also discussed.

1. Introduction

The OPAL microvertex detector has reached its completion. Last year no new developments were started on this detector and only a very small amount of hardware work was done to complete the project. At the moment the microvertex detector plays an important role in the harvest of LEP2 data and therefore, remains closely monitored for data quality. A fully detailed description of the OPAL microvertex detector can be found in Ref. [1]. Here only a short account is given of the operating experience of this detector in the past year and its status today.

A detailed description of the radiation monitoring and beam dump system of the OPAL microvertex detector is given in Ref. [2]. Emphasis is given to the operating experience with this system and several examples of incidents will be discussed.

2. Status of the OPAL Phase III microvertex detector

In this section we will start with a short reminder of the OPAL microvertex detector, followed by a brief account of the operational experience in the past year and some relevant results. This section concludes with a short discussion of the state of the OPAL microvertex detector today.

2.1. The OPAL Phase III microvertex detector

The Phase III OPAL microvertex detector is built up of ladders that contain the silicon detector

*Correspondence address: PPE division, CERN, CH–1211 Geneva 23, Switzerland, E-mail: Sijbrand.de.Jong@cern.ch.

0168-9002/98/$19.00
PII: S0168-9002(98)00713-X

wafers and the signal multiplexing electronics. The overall layout of the detector can be seen in Fig. 1.

Two types of ladders are used: long ladders that contain three wafers lined up one after the other and short ladders that contain two of these wafers. The long (short) ladders consist of three (two) pairs of back-to-back glued wafers supported by a glass plate with Kevlar/epoxy stiffeners. A metal print on the glass plate arranges the fanout of the z wafers from the long side of the ladder to the short side. On one side of the ladders the front-end electronics is mounted on beryllia (BeO) ceramic substrates.

The ladders are connected via a small cable to InterConnect Ring (ICR) cards, which contain the repeater electronics and allow for a transition to thicker cables. On the outside of the OPAL magnet return yoke patch panels are situated that allow the cables to be rearranged and from there thicker cables run to the counting room that houses the processing electronics and power supplies.

The detector is cooled with water in a closed circuit, that is underpressured at the detector and is kept in a dry atmosphere by flushing nitrogen through the enclosing volume. A summary of some performance parameters is given in Table 1.

2.2. Operational experience and data quality

The Phase III detector has performed very stably and reliably in 1996, the first year of its operation. The efficiency has been optimal with no failures during physics experiments. It was therefore decided

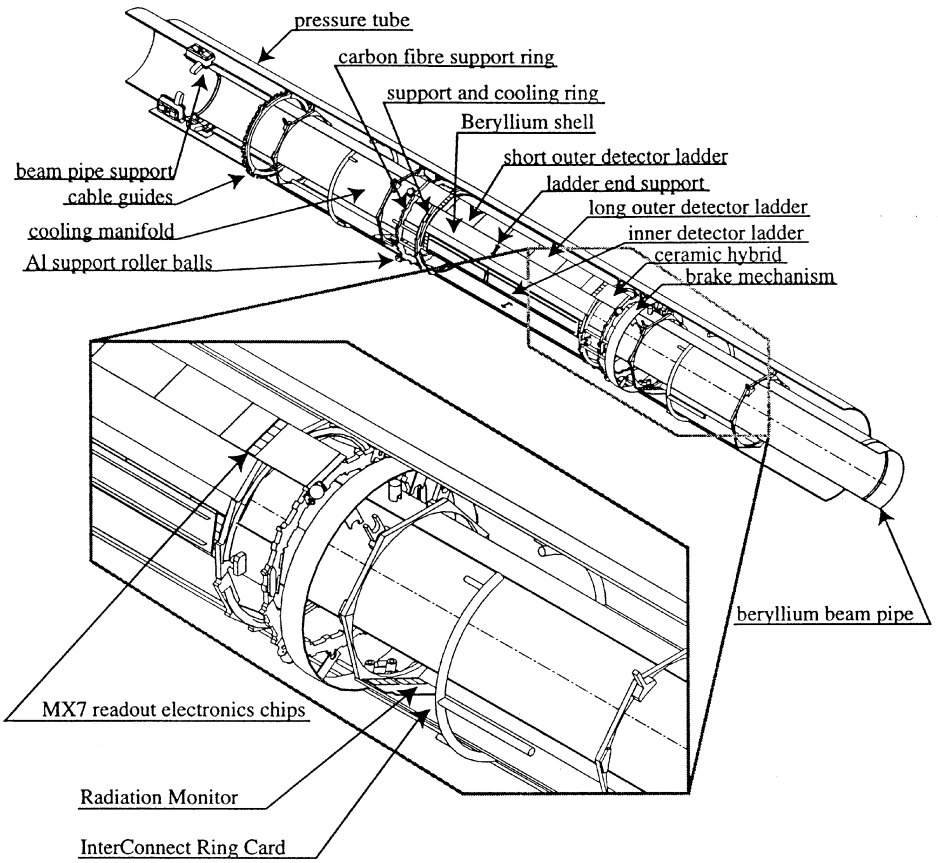

Fig. 1. The OPAL microvertex detector with a blow up view of the new radiation monitoring cards and an indication of their position with respect to the rest of the OPAL microvertex detector.

Table 1
Characteristics of the μVTX3 OPAL microvertex detector

Phase III detector parameter	Value
Number of ladders per layer	12 (inner), 15 (outer)
Effective radius of layer	60.5 mm (inner), 73.8 mm (outer)
Maximum $\|\cos\theta\|$ acceptance	0.93 (inner), 0.89 (outer)
ϕ Acceptance	97.8% (inner), 99.6% (outer)
Average material thickness	1.5% X_0 at normal incidence
Strip biasing method	FoxFET (gated reach-through channel)
2 Coordinate detection	Back-to-back ϕ and z single-sided detectors
z Readout scheme	Aluminium or gold printed circuit on 200 μm Thick glass
Number of active channels	65 502
Readout chip, noise, power	MX7, 350e + 15e/pF, 2 mW/channel MX7-RH, 320e + 21e/pF, 2 mW/channel
Signal-to-noise ratio	24 (ϕ) and 20 (z) (long ladders), 29 (ϕ) and 25 (z) (short ladders)
Radiation hardness	~ 500 Gy (MX7 chip)
Cooling method	Water cooling, under-pressured at detector
Fraction of good channels	≈ 99%

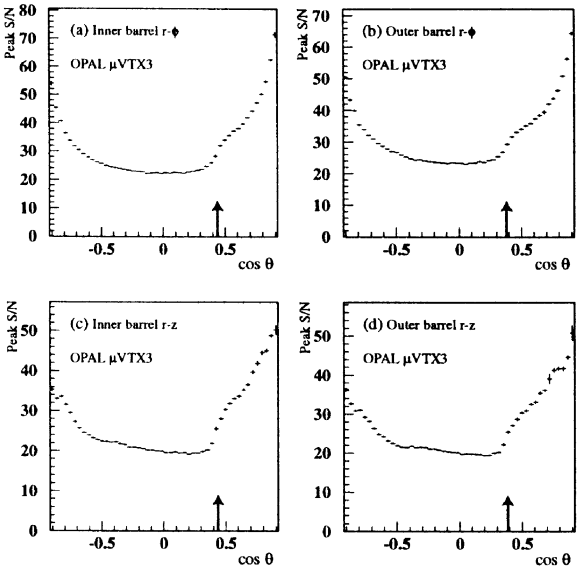

Fig. 2. Signal-to-noise (S/N) ratios for (a) all r–ϕ readout channels in the inner barrel, (b) all r–ϕ readout channels in the outer barrel, (c) all r–z readout channels in the inner barrel, and (d) all r–z readout channels in the outer barrel. The $\cos\theta$ value of the point where the long and short ladders join is indicated by the arrow.

not to shut down the detector for maintenance and only minimal work was done on the cables to allow access to other parts of the detector during the 1996–1997 LEP shutdown period. The detector performance in terms of signal-to-noise ratio is illustrated in Fig. 2. For perpendicularly incoming minimum ionising particles the most probable signal-to-noise ratio is about 24:1 for r–ϕ and 20:1 for r–z. The single-hit matching efficiency for isolated high momentum muon tracks was found to be 97% with a 94% efficiency to match two microvertex hits to such tracks. The impact parameter resolution for $e^+e^- \to \ell^+\ell^-$ events is illustrated in Fig. 3. The impact parameter resolution values of 18 μm for d_0 and 24 μm for z_0 were essentially limited by the number of tracks available to calibrate the OPAL wire chambers at LEP2. However, this performance is quite adequate for the physics analyses to be performed.

The LEP2 operation has led to a much increased off-momentum particle background causing many triggered events from beam–wall interaction. These beam–wall events often have many tracks that cross the microvertex detector at very small angles, leaving long paths of ionisation and many strips hit. The online software tends to absorb these events as redefinitions of the pedestal values, thereby introducing a bias. To avoid this situation, only events without a track trigger are now used to update the pedestal values. In practice, this amounts to roughly half the triggered events.

Since the start of 1997, there have been two ladders for which the ϕ side does not give sensible readout information. The suspicion is that there is a failure, either short or open, just in front of the differential amplifier on the ICR card, which is impossible to reach without dismantling a substantial part of the OPAL detector. This failure results in a solid angle area of 1.7% of 4π, or about 2% of the phase space nominally covered by the microvertex detector, which is now covered by only one

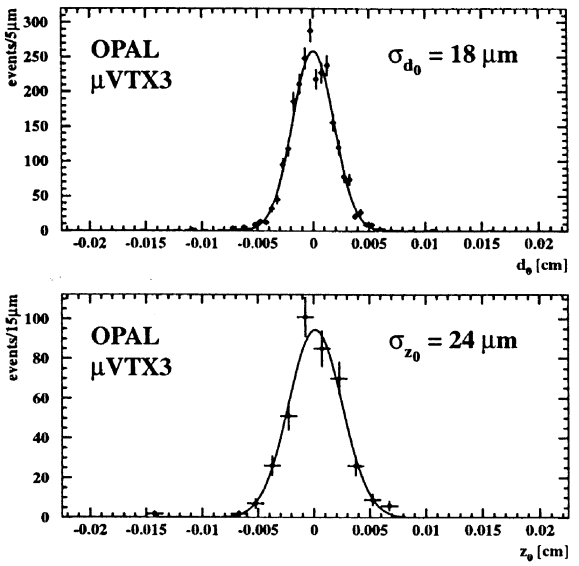

Fig. 3. Impact parameter distributions in the plane perpendicular to the beam axis (d_0) and in the direction of the beam axis (z_0) for $e^+e^- \to \ell^+\ell^-$ (ℓ = e,μ) events taken in 1996. The points with error bars are the data and the full line is a gaussian fit.

layer instead of two layers of silicon microstrip detectors. The z coordinate measurement for these ladders is fine. Since the internal alignment of the detector did not change with respect to 1996, the matching ladders on the other barrel are well aligned and the loss of data quality is very small. This failure triggered a change in the hit to track matching software. Previously, z hits that did not have a corresponding ϕ hit were not considered in the track fit. This requirement has now been lifted. The result is that the influence on physics analyses is minimal and it is therefore decided not to extract the detector for repair in the next winter shutdown.

3. Radiation monitoring and beam dump system

The LEP environment does not pose much concern on radiation damage in general. Therefore, for the design of the OPAL microvertex detector, initially, radiation from the LEP machine was not taken as a serious constraint. However, when operating the detector it was found that the radiation is not far away from the levels that can be maximally tolerated, specifically by the radiation soft version of the MX7 chip. To improve on that situation a radiation hard version of the MX7 was developed and used on the short ladders, which were the parts to be most recently constructed. The long ladders have been carried over from the Phase II to the Phase III detector and remain equipped with the radiation soft version of the MX7 chip. The latter chip defines the lower limit of the radiation tolerance of the OPAL microvertex detector. The radiation soft version of the MX7 chip can take up to about 30 Gy without loss in signal over noise, while at 300 Gy the loss in signal over noise is about 20%, as measured with a 10 mCi ^{90}Sr source.

At LEP1 radiation doses are accumulated to the order of 1 Gy for each functioning year. The LEP2 environment was expected to produce more radiation, with estimates ranging up to a tenfold increase. Meanwhile the observation is that in the first full year of LEP2 running, in 1996, the radiation levels were comparable or even less than those at LEP1.

From the beginning, a radiation monitoring system was installed with the microvertex detector. The original radiation monitors consist of four solar cells which are left unbiased and on which the charge generated by radiation is measured. This charge is converted to a frequency at the patch tower and transported to the control room where it is converted to a voltage that is measured by an ADC. The use of a frequency to transport the signal makes the signals robust but slow and the rise-and-decay time constant is of the order of 1 s. The total amount of charge that was generated is conserved by the signal treatment, making this system useful to measure total radiation doses and making a history profile accurate to 1 s. Remarkably enough, a small fraction of solar cells have a very small temperature sensitivity. These were selected for use in the experiment after detection of fake radiation due to temperature variations had caused problems and could not be easily corrected for by software (due to hysteresis in temperature versus charge creation, the absence of thermistors very close to the solar cells and limitations in the accuracy of temperature monitoring.) The solar cell radiation monitoring system is sketched schematically in Fig. 4.

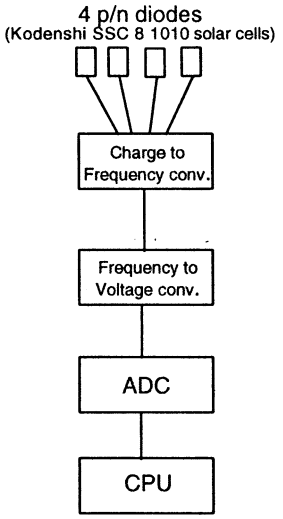

Fig. 4. Schematic layout of the first radiation monitoring system deployed by the OPAL microvertex detector.

3.1. System description

After an incident in which 200 microplex channels were destroyed by a pencil like beam, it was realized that very fast detection of radiation and response to fast rising radiation by means of a beam dump is desirable. For this purpose a new set of radiation monitors was developed and installed. These new radiation monitors use $8 \times 8\,\mathrm{mm}^2$ test diodes from the detector wafers. A number of these diodes are connected in parallel and reverse biased. The signals from these diodes are proportional to the charge liberated in the diodes, which in turn is proportional to the radiation dose. These signals are preamplified and transported to the counting room. In the counting room the signals are split in a signal path that is shaped with a time constant of the order of 1 s for integrated dose measurements and a fast signal that is used in a beam dump circuit that responds to very high doses in very short time intervals. The positioning of the detector cards with the silicon diodes can be seen in Fig. 1.

After various trails in OPAL with the new radiation monitors it was realized that they observe significantly more radiation than the old solar cells. This can be explained by several facts. The solar cells have a lower intrinsic sensitivity, because they are unbiased. But even more important, the solar cells are positioned on the ICR cards facing away from the beam pipe. Therefore, certainly for small-angle tracks, they have a significant amount of material between the sensors and the beam. The new radiation monitors are mounted on the side of the ICR cards facing the beam pipe and have very similar exposure to the beam as the inner barrel ladder detector wafers. The response to off-momentum particles and particle showers is not significantly different for the old and new monitors, but the response to synchrotron radiation differs by more than a factor of 10.

It was also realized that it is impossible to obtain at the same time an accurate integrated dose measurement, for which sensitivities of about 0.50 mGy/h are desirable, and a beam dump system for which the lowest sensitivity is 10 mGy/s. Therefore, the new system was further upgraded to use in addition to the amplified signal from the front end cards, also the signal over the filtering capacitor for the backplane bias voltage (capacitors C1 and C11 in Fig. 5.) This allows to have a total dynamic range of about 10^8 by combining the two signal paths. The final front end card is shown in Figs. 5 and 6.

To avoid saturation problems due to high leakage currents, the silicon diodes for the radiation monitor cards were subjected to stringent leakage current stability tests. Only very stable diodes were retained for use in the radiation monitors.

Both the signal from the two-stage amplifier (amplifier signal) as well as the signal from the filtering capacitors (backplane signal) of the radiation monitor front end cards are treated similarly in the counting room. The signals are terminated by 120 Ω over a large capacitor and the signal over the termination resistor is AC coupled to a differential amplifies. The RC time of the capacitor at the input of the differential receiver amplifier is chosen such that the input signal is differentiated. The differentiated signal is then rectified. This rectified differentiated signal is still proportional to the charge created in the diodes on the front end card, although the constant of proportionality depends critically on the signal shape that results from the ensemble

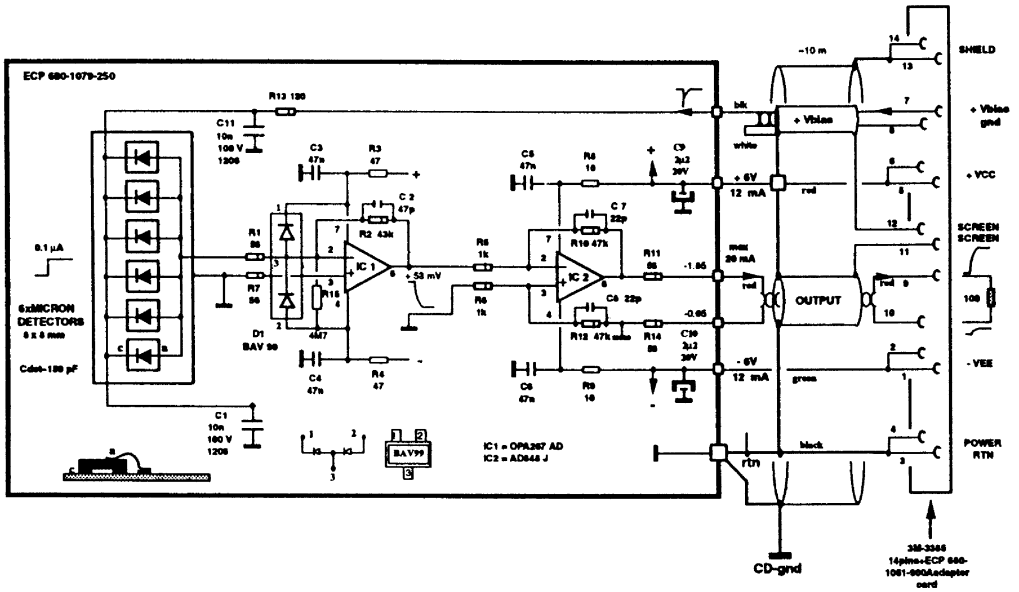

Fig. 5. Schematic diagram of the radiation monitor front end card.

of amplifiers. This is not a problem as the properties of this ensemble of amplifiers are very stable and the channels are calibrated one by one using test input signals. The rectified differentiated signal is fanned out to both a shaper with an RC time of 1 s for an integrated dose measurement as well as to a beam dump module.

The beam dump module integrates the fast rectified differentiated signal, but releases the integrated charge at a constant, but adjustable, rate. This decay rate is currently set to 10 mGy/s. This means that radiation levels under 10 mGy/s will remain unnoticed by the beam dump circuit. Levels over 10 mGy/s will integrate up and when the integral exceeds a certain level an alarm or dump bit will be set. Presently the alarm and dump levels are set to 5 and 10 mGy. The beam dump circuit derives a beam dump signal from the coincidence of at least one channel above dump level and a settable number (currently two) of channels above alarm level.

The radiation monitor and beam dump system are set up independently for both the left- and right-hand sides of the detector.

3.2. Operational experience

Parts of the microvertex detector, especially many of the long 3-wafer ladders, have been operational in OPAL since 1993. It is therefore relevant to estimate the radiation dose they received so far. In 1993 and 1994 only the radiation monitoring system based on the solar cells was available. From 1995, the new radiation monitoring system was available in addition. However, in 1995, the electronics was DC coupled to the sensors and a number of sensors failed completely to give a measurement due to large leakage currents. The measurements for the remaining sensors were very sensitive to the temperature at the sensor. Most of this sensitivity could be taken out by software temperature corrections, but some residual inaccuracy remained due to hysteresis effects when the temperature is cycled. In 1996, the new system as described in this paper was operational and proved to be very stable without the need for temperature corrections. The integrated radiation dose for 1993 and 1994 has been estimated by scaling the dose that

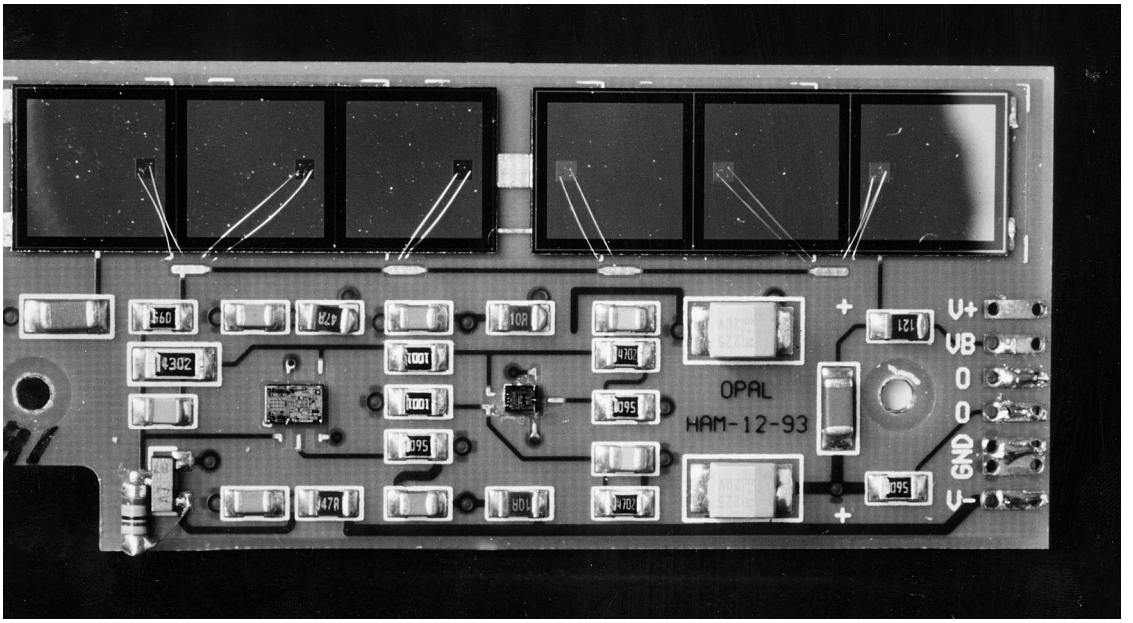

Fig. 6. Photograph of the radiation monitor front end card.

was measured with the old solar cell system, using scale factors between that system and the new system that were determined in 1995 and 1996. The total dose for 1993 and 1994 is thus estimated to be 4.8 Gy. In 1995 the total radiation dose was measured to be 1.4 Gy, while in 1996 this was 0.26 Gy.Fig. 7 gives the average and highest radiation dose received in 1996. All these doses are averaged over the 14 sensors close to the microvertex detector. The total average dose received is thus about 6.5 Gy for most of the long ladders and less for the short ladders. In general, the local dose is much more for some parts of the detector and an estimate of the highest dose received by any part of the detector is about 14 Gy. Knowing that the radiation softest part of the detector, the MX7 microplex chips of the long ladders, can take at least 30 Gy, before starting to deteriorate, there is no cause for concern yet. Especially not since the trend when going from LEP1 operation to LEP2 operation seems to be a decrease in radiation rather than an increase.

The beam dump system has been fully operational this year, except that the LEP interlock was

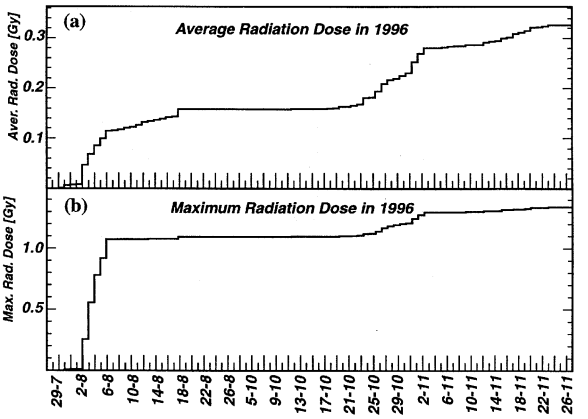

Fig. 7. Average and highest radiation dose received in 1996. The date is given in day of the month and month on the x–axis.

by-passed. This means that in case a beam dump signal was produced by the system, it did not dump the LEP beams, but it was transmitted to the OPAL control room and all procedures were followed as if the beam had been dumped by the system. Also last year a prototype beam dump

system similar to this years was operated, in a similar way for more than one month. The joint experience of these two trail periods is that beam dumps that would have been triggered by this new system were always in situations in which the beams were lost after a short time anyway. However, in some cases the radiation that was received by the OPAL microvertex detector could have been significantly limited if this beam dump system would have been active. A formal request has been put forward to the LEP machine group to enable the possibility to dump the beams by this system.

3.3. Examples of radiation incidents in OPAL

In the first example traces of a multichannel analyser connected to the radiation sensors are shown for various incidents in Fig. 8. This illustrates the typical range of time constants involved in radiation incidents, which goes from several milliseconds to nearly a second.

The second example shows that radiation incidents can be very directional. In Fig. 9 the sensors 2 on both the left and right side of the microvertex detector see a very large radiation dose and all

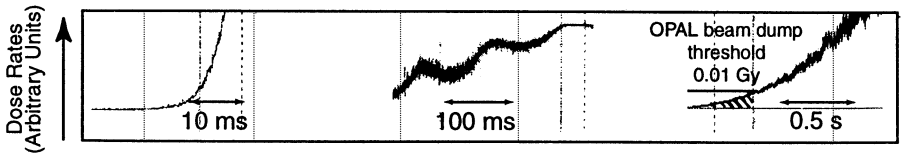

Fig. 8. Examples of time structure for different radiation incidents.

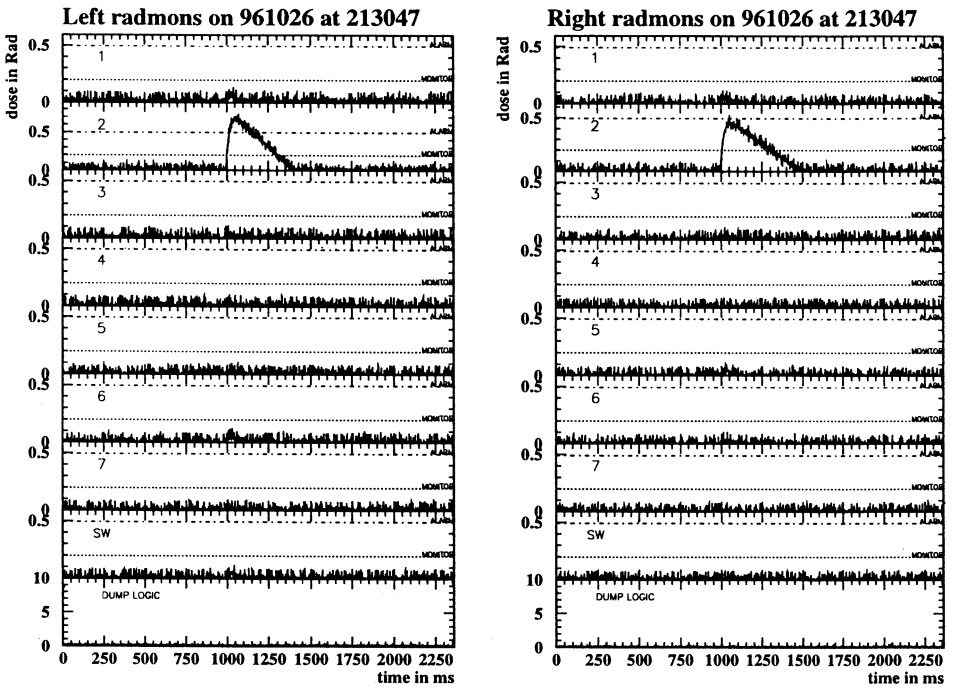

Fig. 9. Example of radiation dose in Rad (100 Rad = 1 Gy) as a function of time in ms. The sensors 1–7 are located near the microvertex detector, on either the left or right side as indicated. Sensors 8 on left and right are mounted in front of the left and right silicon/tungsten luminometer, respectively. This incident occurred on 26 October 1996 at 21:30pm.

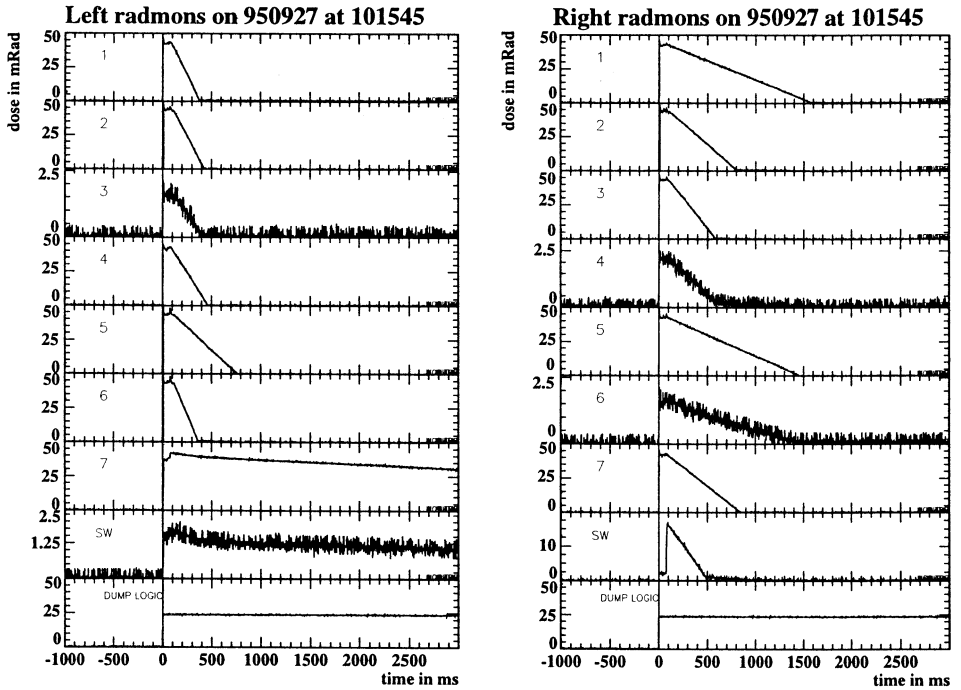

Fig. 10. Example of radiation dose in mRad (100 mRad = 1 mGy) as a function of time in ms. See caption of Fig. 9 for explanations. This incident occurred on 27 September 1995 at 10:15am.

other sensors show no significant radiation. This means that the radiation must have been localised in a sector in azimuthal angle of less than 50°.

In OPAL there is another beam dump system active that is designed to protect the silicon/tungsten luminometer. This system acts on extremely high currents induced in silicon wafers at a depth of several radiation lengths into the calorimeter. The need for a separate system for the microvertex detector is made clear in Fig. 10. It can be seen in this figure that a sudden and large dose of radiation starts to be absorbed by the microvertex detector sensors (1–7) at relative time 0 ms. The silicon/tungsten luminometer only starts to see large radiation about 90 ms later, as shown by the sensor 8 on the right side, which is mounted in front of the luminometer. In fact, at this later time the luminometer beam dump system dumped the beams and the radiation disappears, resulting in the linear decay of the signal on all sensors. The microvertex sensors stayed in saturation for the entire 90 ms period between the start of the incident and the firing of the luminometer beam dump. Clearly the accumulated radiation could have been limited by a large fraction if the microvertex sensors would have triggered a beam dump.

4. Conclusions

Since 1991 a silicon microvertex detector is operational in the OPAL experiment. The microvertex detector has gone through three phases of increasing sophistication and coverage of solid angle. The presently installed Phase III microvertex detector is the final phase and will serve until the end of the LEP era (which is foreseen around the year 2000.) A sophisticated radiation monitoring and beam dump system has been installed and commissioned to safeguard the detector from radiation damage. This system has been demonstrated to monitor long-term radiation dose accurately and at the same time to be capable of dumping the LEP beams within a millisecond in case of extremely

high radiation levels. The OPAL physics programme has greatly benefited from the presence of the microvertex detector. For the LEP2 high energy running the main function of the microvertex detector will be the recognition of Higgs particles that decay in b quarks. It is hoped that soon examples of positive identification of Higgs bosons with the help of the microvertex detector can be shown.

Acknowledgements

In addition to acknowledging the hard work of the entire OPAL microvertex detector group, I want to specifically mention the calibration and alignment work of Michael Hapke. The recent final upgrade of the radiation monitoring and beam dump system has been done largely by Homer Neal and Sylvie Braibant, while the initial start of the project and many of the basic ideas have been delivered by Jan Lauber, Alan Honma and Otmar Biebel. Eduardo do Couto e Silva, Ronald Shellard and the other organisers of the VERTEX97 workshop are warmly thanked for bringing us together in Brazil and organising a smooth and stimulating workshop.

References

[1] P.P. Allport et al., Nucl. Instr. and Meth. A 403 (1998) 326.
[2] O. Biebel et al., Nucl. Instr. and Meth. A 403 (1998) 351.